Deep Learning based Millimeter Wave Beam Tracking at Mobile User: Design and Experiment

Pengbo Si*, Yu Han*, and Shi Jin*
*National Mobile Communications Research Laboratory, Southeast University, Nanjing, China
Emails: {220180882, hanyu, jinshi}@seu.edu.cn

***Abstract*—Beam tracking is of great interest in millimeter wave (mmWave) communication systems, because it can significantly improve the user's received signal power for high-speed communications. However, the existing algorithms have high beam training overhead, and it is difficult to achieve real-time tracking of the beam. This paper proposes a novel beam tracking for mmWave systems based on deep learning (DL) network. Specifically, considering the attribute of the user's mobile behavior, beam training is performed at several consecutive moments. Then, the designed long short-term memory (LSTM) network utilizes historical beam measurements to predict the best future communication beam. In addition, in order to make the network applicable in different scenarios, we also add a switching module to adjust the output according to the characteristics of the current environment. The over-the-air (OTA) results demonstrate that the network performs well and is robust to various scenarios.**

***Index Terms*—Deep learning, mmWave, beam tracking, OTA**

I. Introduction

Millimeter wave (mmWave) has been identified as a key technology for the next-generation wireless communication due to its ability to provide huge bandwidth that can produce unprecedented peak data rates [1]. However, compared with current cellular systems, communications at mmWave frequencies are challenging since the signal propagation encounters different problems, such as higher free space path loss due to the Friis' Law [2], which further leads to severer blockage. Fortunately, owing to the millimeter-scale signal wavelength, phased antenna arrays can be deployed in transceivers to provide highly directional array gain and compensate the great loss through beamforming. Since the communication link is established on basis of the narrow beams at both the transmitter and the receiver, it is necessary to perform beam alignment in order to achieve the strongest received power.

Existing algorithms for beam alignment are basically divided into two categories: codebook-based and non-codebook adaptive beamforming. The second category is complicated and difficult to apply in practice. Therefore, the codebook-based category is drawn with more interest. There are different approaches to perform codebook-based beam alignment. For example, in order to shorten the beam training time, hierarchical beam scanning [3], which has been applied in IEEE 802.11 ad, can be used to avoid exhaustive search. Another approach is black box function optimization. In [4], the beam alignment process aimed at determining the best beam pair for communication is expressed as a global optimization problem in a two-dimensional plane formed by the beam pattern index. A pattern search algorithm was then used to perform the beam search. Furthermore, side-information, such as position information can be utilized to increase the beam alignment efficiency. [5] proposed an approach that can realize multi-Gbps data transmission service by applying the effective position information provided by train control systems to the beam alignment design. Recent advances in deep learning (DL) have sparked interest in introducing DL technologies into communications, and DL has been applied to beam alignment. In [6], the beam prediction problem was transformed to image classification tasks that neural networks excel at, and the transfer learning method is utilized to fine-tune the trained network. Unfortunately, the proposed method relies on additional sensors, and the structure of neural network is complex, causing high computational overhead.

This paper effectively applies DL in practical mmWave communication systems. We propose a novel beam alignment algorithm, which can be deployed at mobile user equipments to predict the optimal beam in real time. Specifically, the neural network algorithm can predict the optimal beam from a predefined codebook by comparing several sets of specific historical measurements, such as signal-noise ratio (SNR) or reference signal receiving power (RSRP) of beams. In addition, the robustness of the algorithm in different scenarios can be improved by adding a switching subnet. OTA test results reveal that the proposed algorithm exhibits much better performance than traditional methods when dealing with mobile user beam tracking problems.

II. System Model

In this section, we will describe the mmWave channel model, the received signal model, and the codebook used in

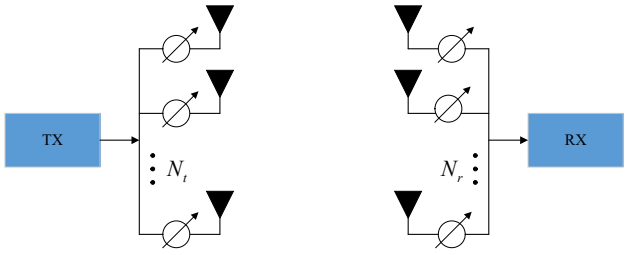

Fig. 1. MmWave system model. The transmitter and receiver are equipped with N_t and N_r antennas, respectively. Phased antenna arrays are used to apply beamforming.

the experiments. More importantly, the specific beam tracking problems studied in this paper will be explained in detail.

The downlink of a mmWave communication system is shown in Fig. 1. The transmitter has N_t antennas and the receiver has N_r antennas. At the transmitter, single-stream data arrives at each antenna through a set of phase shifters, and is then transmitted over a wireless channel. While at the receiver, the data received by the antennas are combined together by a set of phase shifters for subsequent baseband processing. The wireless channel can be given by

$$\mathbf{H} = \sum_{l=1}^{L} \alpha_l \mathbf{a}_r(\phi_l^r)\mathbf{a}_t^H(\phi_l^t), \tag{1}$$

where L denotes the number of paths and α_l is the complex channel gain of the lth path. $\mathbf{a}_t(\phi_l^t)$ and $\mathbf{a}_r(\phi_l^r)$ are the transmit and receive array response vectors, respectively, and they are determined by the antenna array topologies. When uniform linear antenna arrays are adopted, the array response vector can be expressed as

$$\mathbf{a}_r(\phi_l^r) = [e^{j\frac{2\pi 0 d \sin\phi_l^r}{\lambda}}, e^{j\frac{2\pi d \sin\phi_l^r}{\lambda}}, \cdots, e^{j\frac{2\pi(N_r-1)d\sin\phi_l^r}{\lambda}}]^T, \tag{2}$$

$$\mathbf{a}_t(\phi_l^t) = [e^{j\frac{2\pi 0 d \sin\phi_l^t}{\lambda}}, e^{j\frac{2\pi d \sin\phi_l^t}{\lambda}}, \cdots, e^{j\frac{2\pi(N_t-1)d\sin\phi_l^t}{\lambda}}]^T, \tag{3}$$

where d represents the antenna element spacing, λ denotes the wavelength, ϕ_l^t and ϕ_l^r are the angle of departure (AoD) and angle of arrive (AoA) of the lth path, respectively.

Considering the fact that both transmitter and receiver use beam steering vectors selected from codebooks, the received signal can be written as

$$y_{m,n} = \mathbf{w}_m^H \mathbf{H} \mathbf{f}_n x + \mathbf{w}_m^H \mathbf{n}, \tag{4}$$

where $\mathbf{n}$ is an additive white Gaussian noise vector, $\mathbf{f}_n \in \mathbf{F}$ denotes the nth beam steering vector, $\mathbf{w}_m \in \mathbf{W}$ is the mth beam steering vector, $y_{m,n}$ is the received measurement, $\mathbf{F}$ and $\mathbf{W}$ are the codebooks of transmitter and receiver, respectively.

In order to limit the power of massive antenna arrays, the actual solution is to equip the RF module with a phase shifter network, other than to adjust both the amplitude and phase. Here, linear beamforming weights are adopted in the codebook. Taking the codebook at the receiver as an example, $\mathbf{W} = [\mathbf{w}_0, \mathbf{w}_1, ..., \mathbf{w}_{M\text{-}1}]$ is a $N_r \times M$ matrix, where M represents the number of beams. The beam steering vector $\mathbf{w}_m$ can be written as

$$\mathbf{w}_m = [e^{j0m\theta}, e^{j1m\theta}, ..., e^{j(N_r-1)m\theta}]^T, \tag{5}$$

where θ is the phase shift unit, and it should be an integer multiple of the resolution of phase shifter. Patterns of beams used in this paper is shown in Fig. 2, where M is equal to 16 and N_r is set as 4.

Due to the high reflection and penetration losses suffered by the millimeter wave signal, most of the energy is concentrated on the line-of-sight (LOS) path, and the energy of the not-line-of-sight (NLOS) path is insignificant [7]. Therefore, the

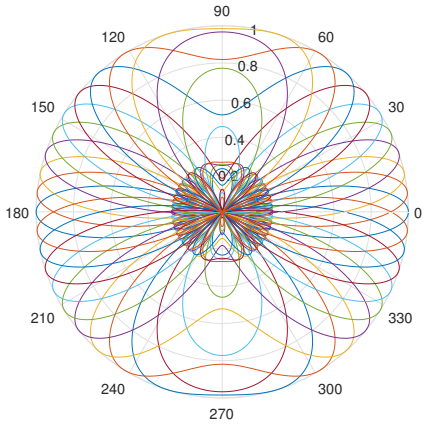

Fig. 2. Patterns of beams in the codebook, where M=16, N_r=4

beam steering vectors at the transceiver must be aligned with the most dominant path. The beam tracking problem is to find the optimal beam steering vector pair $(\mathbf{w}_m, \mathbf{f}_n)$ from the pre-defined codebooks to maximize the power of the received signal.

When the user moves or rotates, the optimal beam pair may change quickly and beam tracking procedure is needed. In this paper, we focus on beam tracking at the user-side. The beam direction of the transmitter is fixed and directed to the receiver, while the beam direction of the receiver is flexible. An optimal beam steering vector is required to be selected from the codebook to establish a high-quality communication link. Therefore the problem is simplified to find the optimal beam steering vector $\mathbf{w}_m \in \mathbf{W}$ to maximize the power of the received signal. However, the fifth generation (5G) cellular network/New Radio (NR) standard limits the time interval for beam measurement, imposing challenges to the beam tracking problem at user-side. Existing algorithms suffer from the large overhead of beam training time, which will seriously affect the beam tracking performance for mobile users. The method to be introduced in the next section can significantly reduce the time consumption and improve the beam tracking ability.

III. Proposed Method

This section presents the proposed framework for beam tracking, including the prediction network and the improved network that can maintain a good performance in various scenarios.

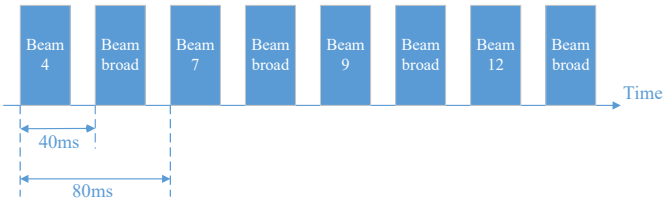

Fig. 3. Beam training diagram

A. Prediction network

We start from the beam training strategy used in this paper, which is closely related to the input of the neural network described later. The number of beam steering vectors of the receiver codebook is 16, corresponding to 16 narrow beams point different directions, as shown in Fig. 2. We consider the configuration of the 5G NR standard, where a beam measurement is performed every 40ms. The beam training timing diagram is shown in Fig. 3.

We decided to continuously measure eight beams as the input of the network. The receiver will perform beam measurements every 40ms, and alternately measure narrow and broad beams, all antennas and only one antenna will be used, respectively. The indice of measured narrow beams are fixed to be 4, 7, 9, and 12, which are demonstrated to be efficient by massive experiments. Innovatively, the introduction of broad beam measurement is the key step, because we found in experiments that there is a relatively stable difference between the RSRP of the broad beam and optimal beam. Therefore, by using the RSRP of the broad beam, the network will obtain a benchmark, which will improve the performance of the network.

Fig. 4 depicts a block diagram of one prediction subnet, it involves a Long Short-Term Memory (LSTM) [8] network, which is accomplished in processing sequence data, and a fully connected deep neural network (FCDNN). The LSTM has four time steps, while three layers are all equipped with 156 hidden units. The activation function used to calculate the candidate value $\tilde{c}_t$ is a ReLU function, $f(x) = \max(0, x)$, to avoid gradients disappearing during training. After that, the output of the last time step of the LSTM network, which is a 156-dimensional vector, is fed into the last one-layer FCDNN. FCDNN has 16 neurons, and the logistic sigmoid function, $f(x) = \frac{1}{1+e^{-x}}$, is used to realize classification function. When we continuously perform beam measurement, the measured value has a time attribute. By inputting the measured values of adjacent moments into the LSTM network in chronological order, it is possible to make good use of the time correlation between the data and improve the prediction ability of the network.

As shown in Fig. 4, the input of the prediction network at each time step is a 17-dimensional vector, which consists of a narrow beam and a broad beam measurements. For example, using the values of the first two beam measurement periods in Fig. 3 i.e., the values of beam 4 and the broad beam, we can form Input 1 as follows. According to the beam index, the narrow beam measurement is placed at the corresponding position, the broad beam measurement is always placed at the end of the vector, and the other positions are set to 0. Based on the above rules, the four time step inputs of the prediction network will be formed by using the previous eight measurements. The 16-dimensional vector output by the prediction network is the probability that the 16 narrow beams will be at the 9th beam measurement, and the optimal beam will be the one with the highest probability.

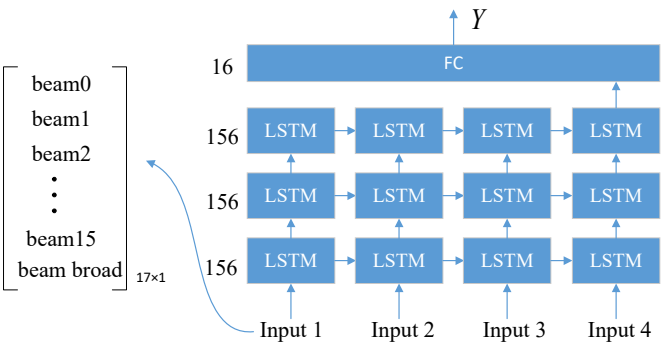

Fig. 4. Prediction network with three-layer LSTM and one-layer FCDNN.

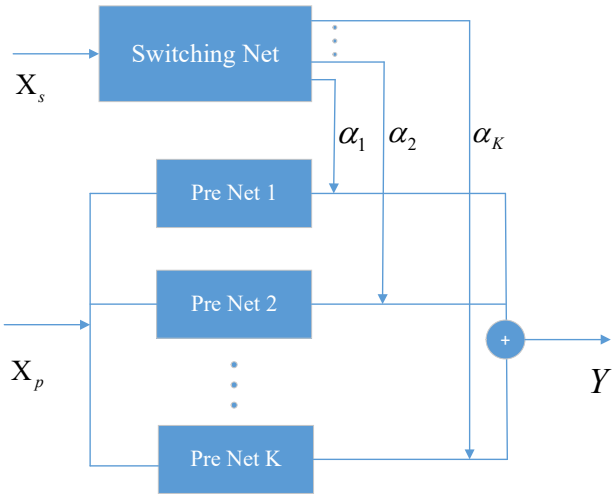

Fig. 5. The neural network architecture includes two types of subnets. Prediction subnets are used to realize the main prediction functions, while switching subnet aims to improve robustness of the network.

B. Improved network

The prediction network can track the beams. However, it is generally trained by the data from a single scenario, and the performance degradation is inevitable if the scenario is different. Since the input of the network is only a measurement of the signal quality of certain beams and the transmission characteristics of millimeter waves are taken into account, if we change the degrees of multipath reflections, the robustness of the network will be reduced.

To resolve the problem, we design an improved network structure by adding a switching subnet. The proposed architecture of the new neural network, as shown in Fig. 5, mainly relies on the original prediction network. The entire network consists of two parts, including a set of parallel prediction subnets to realize the pivotal beam tracking function and a switching subnet [9] to improve the robustness of the algorithm in different K scenarios, where the Pre Net k represents the prediction network trained using data from kth scenario.

As shown in Fig 6, the switching subnet involves a two-layer FCDNN with 32 and K neurons on the two layers,

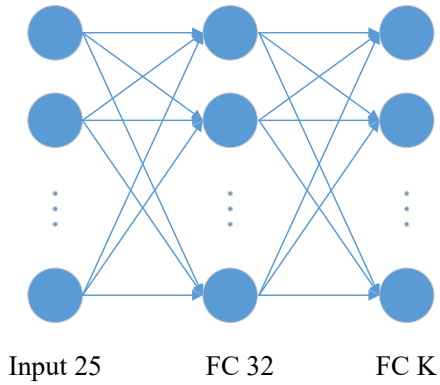

Fig. 6. Switching subnet is used to maintain network performance in different scenarios. It is a two-layer FCDNN with 32 and K neurons in the two layers, respectively.

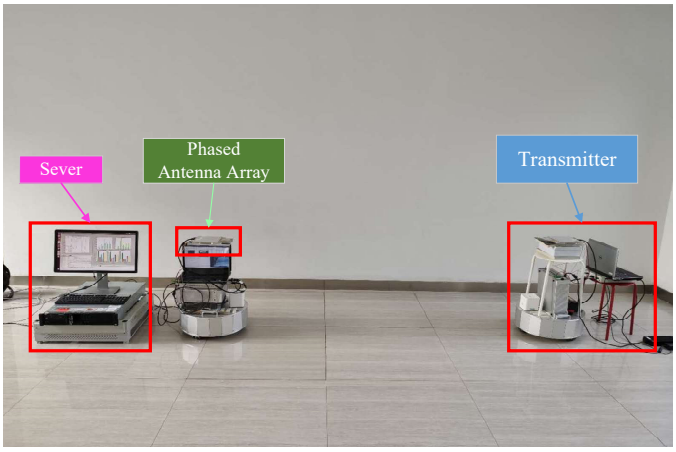

Fig. 7. OTA test system in scenario2.

respectively. The input is the 25 broad beam measurements over the last 100 beam training periods and the output is a K-dimensional vector used as the multiplicative coefficients of the output of the subsequent prediction subnets. The input is different from that of the prediction network because: a) The user's environment does not switch quickly and frequently, so the switching network can use a longer period of beam training values to obtain better performance. b) In different scenarios, the measured value of the broad beam has obvious differences, and its changes are relatively stable in the same scenario; therefore, it can be used to represent the scenarios well. Although the network is called switching net, the coefficients are actually the result of the softmax layer, which are distributed between 0 and 1. The reason for using a switching subnet and multiple prediction subnets in parallel is that we can quickly and conveniently add prediction subnet modules for different scenarios according to demand, and only a mixed data set is required to converge a much smaller switching subnet rather than prediction network.

By adopting such a network input structure, there are the following two advantages: a) Only the measurement value of the specified beam is required, no additional equipment is needed such as sensor, and no interaction with the base station is needed to shorten communication overhead. b) The characteristics of the four time step inputs of prediction network are consistent, so historical data can be used through time sliding windows to reduce each network prediction cycle from eight to two beam training periods.

The training is conducted with a cross-entropy loss [10] given by:

$$L = \sum_{m=0}^{M-1} p_m \log(q_m), \tag{6}$$

where q_m is the output of neural network and p_m is the probability distribution of real data induced by a softmax layer.

Suppose there are two different scenarios, including scenario 1 with rich reflection paths and scenario 2 with few reflection paths. We use the data from scenario1 and the above loss function L to train the Pre Net 1 separately and fix it, and then Pre Net 2 performs the same operation. After that, two prediction subnets are connected in parallel and a switching subnet is added, which will be trained by mixed data set.

IV. EXPERIMENTAL RESULTS

A. System Setup

In this section, we use a 5G NR based end-to-end real-time mmWave prototyping system [11], which adopts orthogonal frequency division multiplexing (OFDM) and frame structure similar to 5G standard, to evaluate the performance of the proposed algorithm in real environments. As shown in Fig. 7, both the receiver and the transmitter contain a universal software radio peripheral reconfigurable I/O (USRP-RIO), which is a software defined radio (SDR) node with 120MHz bandwidth, an mmWave phased antenna array used to support beamforming, and a laptop to manipulate the SDRs. In addition, the receiver is equipped with a server to run the neural network. The transmitting mmWave frequency point is set to 28 GHz. Both the receiver and the transmitter use four antennas in the phased antenna array to implement beamforming, and the codebook used is a linear codebook with 16 beam steering vectors, which has been presented in Fig. 2.

Fig. 8 illustrates the frame structure adopted by this prototyping system. One 10ms radio frame includes ten subframes, and eight slots form a subframe. The subcarrier spacing is

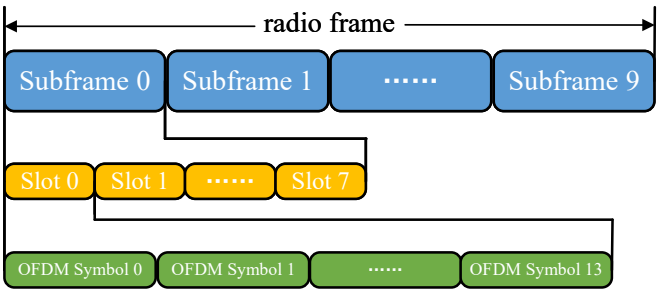

Fig. 8. Frame structure for transmitting.

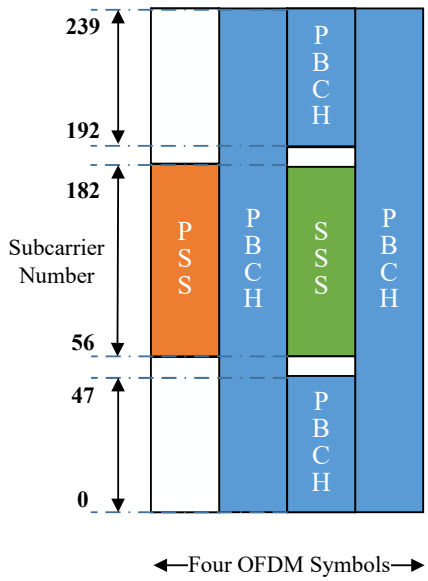

Fig. 9. SSB structure.

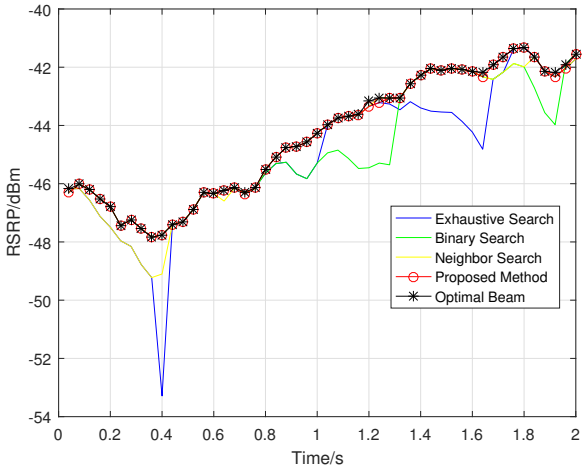

Fig. 10. The RSRP of the beams predicted by four algorithms and that of the optimal beam. This experiment was performed in scenario 1, and the rotational speed is 20°/s.

120KHz. One slot contains 14 OFDM symbols. The transmitter will continuously transmit the above radio frames, and the receiver can perform beam measurement based on several specific OFDM symbols.

It is defined in the 5G standard that beam measurement is performed according to a synchronization signal block (SSB), a continuous four OFDM symbols block. One synchronization signal block corresponds to one beam measurement, as shown in Fig. 9. In addition, SSB, as its name indicates, also plays the role of synchronization signal. One SSB occupies four OFDM symbols in the time domain and 240 subcarriers in the frequency domain, including primary synchronization signal (PSS), secondary synchronization signal (SSS), and physical broadcast channel (PBCH). The PSS generated by the m sequence occupies 127 subcarriers on the first OFDM symbol, which will be detected by the receiver using the autocorrelation operation to determine the starting position of the radio frame. The SSS on the third OFDM symbol will be used to measure RSRP, which is the beam measurement value in this paper. RSRP is defined as the linear average power of the resource elements carrying SSS, and its unit is dbm. First, the receiver finds the position of the PSS by using an auto-correlation operation, and then obtains the position of SSS to calculate RSRP as the current beam measurement value.

In the experiments, the transmitter is fixed and points to the receiver, and the receiver rotates at a constant speed within the range of AoA$\in [-60°, 60°]$. The receiver will measure the RSRP of a specific beam every 40ms, which can be calculated according to the pre-set frame structure, and send it to the neural network in the server. The measurements of narrow beam and broad beam are performed alternately, when measuring the broad beam, the receiver uses only one antenna to receive.

We collected 80,000 and 120,000 samples in scenario 1 with multipath reflections and scenario 2 with few multipath reflections, respectively. Training and test sets account for 70 and 30, respectively.

The set of variables is optimized by the Gradient Descent optimizer. The batch sizes of prediction subnet and switching subnet are both 128 and the numbers of epochs are 500 and 50, respectively. Moreover, the initial learning rates of two kinds of subnets are both 0.1, and it will decay by 0.9 each 7000 turns.

B. Experiment Results

We compare the performance of the proposed algorithm with exhaustive search, binary search, and neighbor search. The exhaustive search sequentially measures the RSRP values of all beams, and selects the optimal beam from them to switch. The binary search divides the current area into two parts, compares the RSRP of the middle beam of the two parts, selects the part where the larger beam is located as the next search area, and iterates until the last beam is found. The neighbor search measures the RSRP of the current beam and its four adjacent beams in order, and selects the largest one as the switching beam.

Fig. 10 show the results in scenario 1 with rich multipath reflections, and the receiver was rotated at a constant speed of 20°/s. The curve of the optimal beam almost coincides with the curve of the proposed algorithm, while the curves of other algorithms are unstable and fluctuate largely the proposed algorithm does not predict the best beam, the RSRP of the predicted beam is close to the optimal.

As shown in Fig. 11, by comparing the beam prediction accuracy of the four algorithms at different rotation speeds, which performed in scenario 1, we find that the method proposed in this letter has significantly better performance than the other three algorithms. In addition, the accuracy of

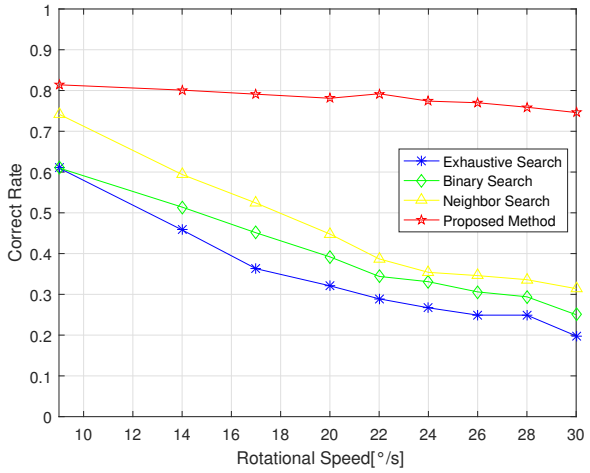

Fig. 11. Optimal beam tracking accuracy of four algorithms at different rotational speeds of UE.

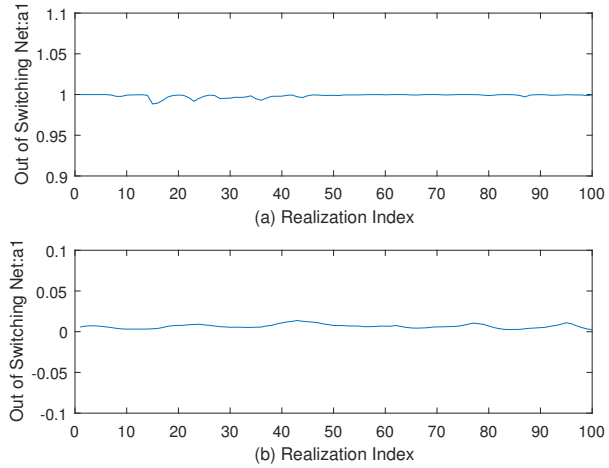

Fig. 12. Output of switching subnet: α_1 in two scenarios.

other algorithms decreases continuously with the increase of the speed, while the accuracy of our algorithm is stable at about 0.8.

Moreover, we also tested the robustness of the algorithm after using the switching subnet in different scenarios. First, we individually examined the output of the switching subnet α_1, which is the weight of prediction subnet 1. Above subgraph from Fig. 12 illustrates the range of α_1 when the network is deployed in scenario 1. Subgraph (b) depicts that α_1 is almost 0, if data from scenario 2 is used. This result shows that the switching subnet can distinguish the scenario well according to the characteristics of the broad beam.

Furthermore, we also compared the performance of the original network to the improved network. From Table I, we can find that when the network training and implementation scenarios do not match, the accuracy will be greatly reduced. By configuring the switching network, the network

TABLE I
ACCURACY OF THE NETWORK IN DIFFERENT SCENARIOS AFTER ADDING A SWITCHING SUBNET.

	Pre Net1	Pre Net2	Switching Net
Scenario1	0.897	0.454	0.904
Scenario1	0.371	0.826	0.822

can maintain its superior performance in different scenarios and improve robustness.

V. CONCLUSION

In this work, we proposed a novel DL network for mmWave beam tracking. In order to improve the robustness of the network in different scenarios, switching subnet and prediction subnet structures are introduced. The OTA test proves that the proposed method has higher accuracy and shorter initial access time than other reference algorithms, and the network structure of the switch significantly improves the robustness of the network.

VI. ACKNOWLEDGEMENT

This work was supported in part by the National Key Research and Development Program 2018YFA0701602, the National Natural Science Foundation of China (NSFC) for Distinguished Young Scholars of China under Grant 61625106 and in part by the NSFC under Grant 61941104.

REFERENCES

[1] R. W. Heath Jr., N. Gonzalez-Prelcic, S. Rangan, W. Roh, and A. Sayeed, "An overview of signal processing techniques for millimeter wave MIMO systems," *IEEE J. Sel. Topics Signal Process.*, vol. 10, no. 3, pp. 436–453, Apr. 2016.

[2] K. Haneda, J. Jarvelainen, A. Karttunen, M. Kyro, and J. Putkonen, "A statistical spatio-temporal radio channel model for large indoor environments at 60 and 70 GHz," *IEEE Trans. on Antennas Propag.*, vol. 63, no. 6, pp. 2694–2704, Jun. 2015.

[3] IEEE 802.11 Task Group AD. [Online]. Available: http://www.ieee802.org/11/Reports/tgad update.html.

[4] B. Li, Z. Zhou, W. Zou, X. Sun, and G. Du, "On the efficient beamforming training for 60 GHz wireless personal area networks," *IEEE Trans. Wireless Commun.*, vol. 12, no. 2, pp. 504–515, Feb. 2014.

[5] V. Va, X. Zhang, and R. W. Heath, "Beam switching for millimeter wave communication to support high speed trains," in *IEEE Veh. Technology Conf.*, Sep. 2015.

[6] M. Alrabeiah, A. Hredazk, and A. Alkhateeb, "Millimeter wave base stations with cameras: Vision aided beam and blockage prediction," preprint, 2019. [Online]. Available: https://arxiv.org/abs/1911.06255v2.

[7] K. Sato, H. Sawada, Y. Shoji, and S. Kato, "Channel model for millimeter-wave WPAN," in *Proc. 2007 IEEE International Symp. Personal, Indoor Mobile Radio Commun.*, pp. 1–5.

[8] S. Hochreiter, J. Schmidhuber, Long short-term memory, Neural Computation 9(1997), 1735–1780.

[9] P. Jiang, T. Wang, B. Han, X. Gao, J. Zhang, C. Wen, S. Jin, and G. Y. Li, "Artificial intelligence-aided OFDM receiver: Design and experimental results," preprint, 2018. [Online]. Available: https://arxiv.org/abs/1812.06638v2.

[10] I. Goodfellow, Y. Bengio, and A. Courville, "Deep learning," 2016, book in preparation for MIT Press. [Online]. Available: http://www.deeplearningbook.org

[11] K. Wang, X. Yang, X. Li, C. Went and S. Jin, "SDR implementation of an end-to-end mmWave testbed based on phased antenna array," in *11th Int. Conf. Wireless Commun. and Signal Proc.*, Oct. 2019, pp. 1–6.